



1,3-Disubstituted-4-Aminopyrazolo [3, 4-d] Pyrimidines, a New Class of Potent Inhibitors for Phospholipase D

Aditya Kulkarni¹, Phong Quang², Victoriana Curry², Renee Keyes², Weihong Zhou¹, Hyejin Cho¹, Jonathan Baffoe¹, Béla Török^{1,*} and Kimberly Stieglitz^{2,*}

¹Department of Chemistry, University of Massachusetts Boston, 100 Morrissey Blvd, Boston, MA 02125, USA

²STEM Biotechnology Division, Roxbury Community College, Roxbury, MA 02120, USA

*Corresponding authors: Béla Török, bela.torok@umb.edu; and Kimberly Stieglitz, kastieglitz@rcc.mass.edu

Phospholipase D enzymes cleave lipid substrates to produce phosphatidic acid, an important precursor for many essential cellular molecules. Phospholipase D is a target to modulate cancer-cell invasiveness. This study reports synthesis of a new class of phospholipase D inhibitors based on 1,3-disubstituted-4-amino-pyrazolopyrimidine core structure. These molecules were synthesized and used to perform initial screening for the inhibition of purified bacterial phospholipase D, which is highly homologous to the human PLD₁. Initially tested with the bacterial phospholipase D enzyme, then confirmed with the recombinant human PLD₁ and PLD₂ enzymes, the molecules presented here exhibited inhibition of phospholipase D activity (IC₅₀) in the low-nanomolar to low-micromolar range with both monomeric substrate diC₄PC and phospholipid vesicles and micelles. The data strongly indicate that these inhibitory molecules directly block enzyme/vesicle substrate binding. Preliminary activity studies using recombinant human phospholipase Ds in *in vivo* cell assays measuring both transphosphatidylation and head-group cleavage indicate inhibition in the mid- to low-nanomolar range for these potent inhibitory novel molecules in a physiological environment.

Key words: chemical biology, drug design, protease and ligands (substrate/inhibitor)

Abbreviations: ARF, ADP-ribosylation factor; diC₄PA, dibutyroylphosphatidic acid; diC₄PC, dibutyroylphosphatidylcholine; LUV, large unilamellar vesicles; MES, 2-(*N*-morpholo)ethanesulfonic acid; PAGE, polyacrylamide gel electrophoresis; PA, phosphatidic acid; PC, phosphatidylcholine; PLD, phospholipase D; PMA, phorbol 12-myristate 13-acetate; POPA, 1-palmitoyl-2-

oleoyl-phosphatidic acid; POPC, 1-palmitoyl-2-oleoyl-PC; Ptd-But, phosphatidyl butanol; SUV, small unilamellar vesicles.

Received 2 August 2013, revised 19 December 2013 and accepted for publication 4 March 2014

Phospholipase D (PLD) is an enzymatically active protein that catalyzes the cleavage of phosphatidylcholine at the ester linkage—releasing choline and phosphatidic acid (PA) (1). Phosphatidic acid is a second lipid messenger located at the intersection of several essential signaling and metabolic pathways (2). Phosphatidic acid is involved in the regulation of essential cellular functions and also mediates enhancement of cell migration. Both increased PLD activity and PLD expression have been observed in a variety of human cancer tissues (3–5). While PLD promotes the ability of cells to initiate defence mechanisms, the inhibition of PLD results in a diminished ability of cells to adhere. Therefore, alleviating PLD activity has recently emerged as a new drug target for human cancer-cell invasiveness (6). Recent studies have also associated human PLD₁ with amyloid precursor protein in Alzheimer's disease (7,8). Hence, a therapeutic strategy, which involves specific inhibition of PLD by small molecules, is highly desirable for the treatment of cancer and Alzheimer's disease.

Mammalian PLD exists in the following two isoforms: PLD₁ and PLD₂. Both of these isoforms have 53% sequence identity and show different modes of activation and functional roles. Recently, extensive efforts have been focused on selective inhibition of one isoform over the other. Figure 1 shows the structures of successful dual- and isoform-selective PLD inhibitors in previous *in vitro* and *in vivo* quantitative cell-based assays. Isoform-selective PLD₁ inhibitor **2** and PLD₂ inhibitor **3** from Figure 1 are structural modifications of dual PLD_{1/2} inhibitor halopemide, **1** (9,10). In order to be PLD₁-selective, the inhibitor requires a (*S*)-configuration on the methyl-bearing carbon adjacent to the amide linkage (9), whereas a PLD₂-selective inhibitor requires a spiro ring fused with the lactam (9,10). These inhibitors were used with the bacterial PLD used in this study for screening and preliminary kinetics, and the two human PLD isoforms overexpressed to test novel inhibitors reported here. The bacterial PLD used in preliminary

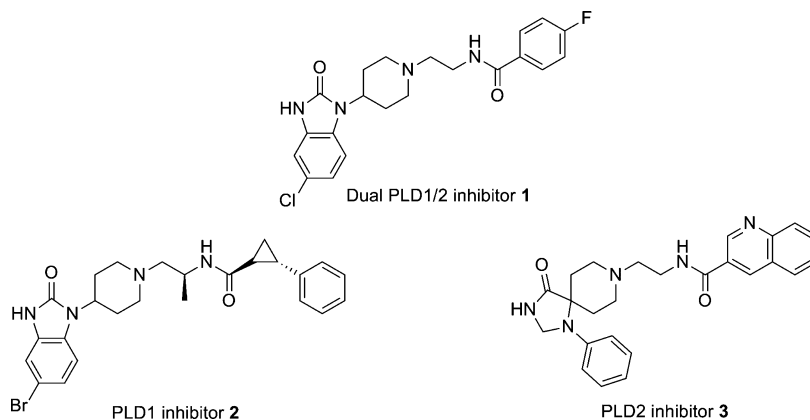


Figure 1: Structures of successful dual and isoform selective PLD inhibitors.

testing of inhibitors is available to purchase from EnzoLife-Sciences and has similar reactivity with the human PLD₁.

This bacterial PLD, from *Streptomyces species strain pmf* (PLD_{sp}) used in this study for preliminary screening of newly synthesized molecules, exhibits a high specificity for phosphatidylcholine (PC) cleavage to generate free choline and PA. The advantage of using this bacterial PLD is that the PLD_{sp} crystal structure has been solved, and the active site contains the highly conserved HKD repeats common within the PLD superfamily, including human and other mammalian PLD's (11). Therefore, when molecules were found to be inhibitory in the *in vivo* and *in vitro* assays with the purified enzyme, molecular docking and viewing the 3D structure may aid in the 'second generation' of drugs design.

Herein, we report highly potent inhibitors of PLD_{sp} and human PLD₁ and PLD₂, which are based on an 4-aminopyrazolopyrimidine core structure (Scheme 1). These enzymes were tested for the inhibition of PLD activity in several *in vitro* biochemical assays using various forms of the phospholipid substrate phosphatidylcholine, from monomer substrate, micelles, mixed micelles, and small unilamellar vesicles (SUV). Preliminary *in vivo* studies were also carried out with various cell lines measuring *in vivo* expression of human PLDs to test for the inhibition of transphosphatidylation activity and PC head-group cleavage (PA production) from whole-cell lipid extraction. 4-Aminopyrazolopyrimidines have earlier been used as tyrosine kinase inhibitors (12) and dual inhibitors of tyrosine and phosphoinositide kinases (13) among other applications. The work presented here expands the application of these molecules as potential potent inhibitors of enzymes in PLD superfamily, which are emerging as targets for cancer research and other human diseases.

The inhibitors designed in this study lack a chiral center or a spiro ring structure, which is attractive from the synthetic point of view. The synthesis was accomplished from eco-

nomically and commercially available starting materials in four steps as shown in Scheme 1. A considerable diversity in the basic core structure could be achieved by using various hydrazines and acyl/aroyl chlorides.

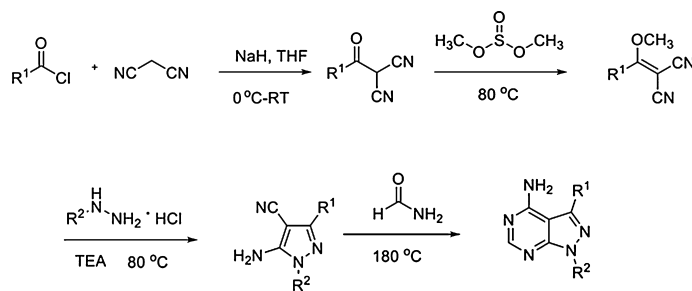
Materials and Methods

Synthesis of inhibitor candidates

All chemicals and solvents used for the synthesis of the inhibitor candidates were purchased from Sigma-Aldrich Corp., St. Louis, MO USA. All compounds prepared were synthesized on the basis of a method described in literature (6,13,14) with minor alterations wherever necessary. A variety of substituted derivatives was synthesized based on the 4-aminopyrazolopyrimidine core structure. The molecules were synthesized in five steps starting from acyl/aroyl chloride and malononitrile. In the first step, the acyl/aroyl chloride was coupled with malononitrile with a simple base-catalyzed addition/elimination reaction. In the second step, enol ether was generated by the addition of dimethyl sulfide. In step three, a pyrazole was synthesized by the addition of a hydrazine. The first three steps were carried out in a one pot manner to get pyrazoles in moderate yields (30–60%). The intermediate was refluxed in formamide to get the final product in high yields (step 4). The identification and purity determination were carried out by mass spectrometry and NMR spectroscopy (¹H and ¹³C) (step 5). Spectra of known compounds were in agreement with the literature data (see Appendix S1).

Preparation of commercially available PLD inhibitors to test bacterial and human PLD enzymes for specificity of inhibition

FIPI (4-Fluoro-N-(2-(4-(5-fluoro-1H-indol-1-yl)piperidin-1-yl)ethyl)benzamide) was purchased from Sigma-Aldrich catalog number F5807. The following PLD inhibitors were purchased from Avanti Polar lipids: #857370 named VU0155056 N-(2-{4-[2-oxo-2,3-dihydro-1H-benzo(d)imi-



R¹ = CH₃, phenyl, 1-naphthyl and 2-naphthyl

R² = H, CH₃, tert-butyl, phenyl, 4-methoxyphenyl, 2-ethylphenyl

Scheme 1: Synthesis of PLD inhibitors.

dazol-1-yl]piperidin-1-yl}ethyl)-2-naphthamide, #857371 named VU0359595(1R,2R)-N-([S]-1-{4-[5-bromo-2-oxo-2,3-dihydro-1H-benzo(d)imidazol-1-yl]piperidin-1-yl}propan-2-yl)-2-phenylcyclopropanecarboxamide, and #857372 named VU0285655-1 N-{2-[4-oxo-1-phenyl-1,3,8-triazaspiro(4.5)decan-8-yl]ethyl}quinoline-3-carboxamide. Lyophilized power was reconstituted in DMSO as a 50X stock. Negative controls were run with all enzymes in the kinetic assays using 2% DMSO with enzymes in the absence of inhibitor to subtract off any inhibition due to DMSO.

Preparation of PLD enzymes for kinetic assays and POPC vesicles

PLD_{sp} from *Streptomyces species strain pmf* was purchased from EnzoLifeSciences catalog number BML-SE301-0025 at 95% pure and dialyzed in 25% glycerol (cryo-protectant) and frozen in -80 °C freezer in small aliquots and was used without further purification for initial screening of small molecules. Human PLD₁ and PLD₂ sequences were purchased Thermo Scientific Inc., (Waltham, MA, USA). The linear sequences were modified with PCR to have EcoR1- and BamH1-flanking sequences that were then digested along with the vector pMET and then ligated into the vector's multiple cloning site (MCS) from the *Pichia* (*P. methanolica*) Kit catalog number K1780-01 (<http://www.lifetechnologies.com/us/en/home.html> accessed 12/16/13). After selecting, scale up, harvesting the vector and insert, the construct was sent out for sequencing (Genewiz, Cambridge, MA, USA) and once confirmed the PLD sequence was intact, it was cut and transfected with electroporation in the yeast cells to select cells, induce expression and harvest PLD proteins. Details of the cloning, purification, and initial characterization of the human PLD₁ and human PLD₂ clones will be published in subsequent publications. Preparation of 1-palmitoyl-2-oleoyl-PC (POPC) vesicles was performed with slight modifications (microscale) as previously described using a sonicator with vesicle samples on ice at 50% duty cycle until the sample was optically clear as possible (OD₅₈₀ < 0.100) (15–17). Dynamic light scattering was used to confirm that vesicles were unilamellar and estimate the size of the SUV and LUV vesicles as previously described (17).

In vitro kinetic assay using soluble substrate diC₄PC for PLD inhibition studies

For initial screening of inhibitors for the inhibition of PLD activity, the pH-stat assay +/- inhibitors was used with the bacterial PLD_{sp} enzyme. About 50 mM NaOH stock solution was standardized with KHP and then diluted in Millipore water (10-fold serial dilutions) and then used to hold the pH constant (at 8.0) in fixed concentrations of 5 mM for diC₄PC, 150 mM NaCl. The diC₄PA product decreased the pH and was in a 1:1 ratio with moles NaOH needed to stabilize the pH at 8.0. This pH is appropriate as the pK_{a2} of the diC₄PA side chain is ~ 6.8 so that all of this product will be titrated at 8.0 (15).

In vitro kinetic assay using [choline-methyl-³H]di-palmitoylPC vesicles for PLD inhibition studies

Compounds that yielded and estimated IC₅₀ of <100 μM were further quantified and tested using a PLD activity assay with human PLD₁ and PLD₂ recombinant proteins measuring the release of [methyl-³H] choline from [choline-methyl-³H]di-palmitoylphosphatidylcholine ([choline-methyl-³H]PC) vesicles as previously described (1,18). Modifications were made to optimize activity especially for the human PLDs. For example, PLD₁ required the addition of cofactor ADP-ribosylation factor (ARF) for optimal activity (18). Briefly, PLD enzymes (at 50 nM) were reconstituted with phospholipid vesicle substrates. Lipid solutions were dried and resuspended, and SUV were prepared by sonication as sited previously. All assays were performed at 37 °C with agitation for 30 min. Reactions were stopped by the addition of trichloroacetic acid and bovine serum albumin. Free [methyl-³H] choline was separated from precipitated lipids and proteins by centrifugation and analyzed by liquid scintillation counting. Raw data are normalized and are presented as relative activity. Experiments are performed in triplicate (18). Once the baseline specific activity was determined for the enzyme, known amounts of inhibitor ranging from 0.1 nM–0.1 mM concentration were added. Initial molecule screening was performed with small molecules listed in Table 2 in the micromolar range (~ 10 data points in duplicate). Then, full duplicate curves were

generated higher or lower than these initial concentrations depending on the efficiency of each individual molecule. The pH-stat assay was run and analyzed as previously described (15–17). Briefly, serial dilutions were made from a small initial volume of inhibitor 0.1 mM stock in 5% DMSO. The IC₅₀ (point of 50% inhibition) was determined graphically by graphing the relative specific activity (Y axis) and inhibitor concentration (X axis) using KALEIDAGRAPH curve-fitting software (2457, Reading, PA, USA). Preparation of POPC vesicles and diC₄Pa was performed with slight modifications (microscale) as previously described using a sonicator with vesicle samples on ice at 50% duty cycle until the sample was optically clear as possible (OD₅₈₀ < 0.100) (15–17).

¹H NMR assay of PLD activity with phospholipid vesicles

¹H NMR (500 MHz) spectra, monitoring choline production, were acquired at a temperature of 37 °C. The parameters used in acquiring spectra, acquisition time, relaxation delay, and pulse width were modeled from those used in previous studies (19). Chemical shifts were referenced to the residual water resonance (before presaturation) as previously described (15–17,19,20). The total volume of each assay sample was 0.250 mL. An initial spectrum was acquired before adding the enzyme and calcium of the prepared phospholipid samples. This served as the zero time control. PLD_{sp} enzymes (2.5 μg/sample) +/- inhibitors were preincubated together for 1.5 h prior to adding to the vesicles. This preincubation of enzyme and inhibitor before adding enzyme to the vesicles for a kinetic run had a marked effect on the efficiency of the inhibitors. After the addition of PLD, an arrayed experiment was carried out for about 1 h. Initial rates were obtained from the progress curve for ~5–30% PC hydrolysis as monitored by the increase in choline N(CH₃)₃ intensity.

³¹P NMR assays of PLD activity with phospholipid vesicles

PLD-specific activities toward short-chain diacylphosphatidylcholine (diC_nPC), including diC₄PC, diC₆PC and diC₇PC, and detergent/POPC mixed micelles were measured by ³¹P NMR spectroscopy in the absence of Ca²⁺ as described previously (20). Samples typically included 10 mM phospholipid in 25 mM buffer (variable depending on pH) in a volume of 0.25 mL, of which 0.05 mL is D₂O. The diC_nPA product was easily detectable as a pH-dependent resonance downfield from the PC resonance (–0.5 ppm). The transphosphatidyl reaction was examined with diC₄PC and CH₃OH as substrates. Most rates were determined from fixed time-point assays (6 to ~25 min) where the PLD_{Sp} reaction was stopped by heating at 100 °C in a hot water bath. Amount of enzymes used was 2.5 mg for each time-point with fresh enzyme added each time, data collected to prevent depletion of enzyme due to sequestering when PA product

was generated. All rates are based on assays run at least in duplicate. ³¹P NMR was also used to quantify PA production in *in vivo* assays with PLD₂ in HEX-293 cells after phorbol 12-myristate 13-acetate (PMA) treatment (19).

Cell culture and transfection

Human embryonic kidney cells (HEK-293) were cultured in DMEM with 10% fetal calf serum and used to study endogenous expression of PLDs as well as transfection with exogenous human PLDs. Cells were grown in 24-well plates. A construct with modified AAV vector, GFP reporter protein and human PLD₁ and human PLD₂ was made. About 0.5 mg of DNA of either construct was used to perform transfection with LipofectAMINE Plus (Invitrogen, Carlsbad, CA, USA). Twelve hours after transfection, the medium was replaced with fresh growth medium, and the cells were cultured for another 18 h before viewing on fluorescent microscope to confirm expression of the construct and proceeding with the *in vivo* assay described briefly below and processing the cells for analysis of PLD activity in the absence and presence of the most potent inhibitors. Preliminary fluorescent imaging of cells and cytology studies of cell morphology with inhibitors introduced herein was performed in an inducible Chinese Hamster Ovary (CHO) cell line cultured in Ham's F12 media and 10% tetracycline free fetal bovine serum (FBS). The CHO cell line has been confirmed to induce (weakly) overexpression wild-type PLD₁ and PLD₂ by adding 2.5 μg/mL doxycycline (Dox) for 24 h in a protocol modified from work previously described (21–24). Preliminary *in vivo* PLD inhibitory assays were carried out under culture conditions as described previously with these cells (21).

PLD *in vivo* transphosphatidylation and head-group hydrolysis (PA sensor) activity assays

In vivo PLD activities were determined using transphosphatidylation to measure the accumulation of Ptd-But in intact cells in a protocol with the new constructs of AAV-GFP-PLD₁ and AAV-GFP-PLD₂ modified from previous research of *in vivo* kinetic studies of PLD (21–24). HEX-293 cells were transfected with PLD₁ +ARF or PLD₂ then incubated with Inh₁ or Inh₂ (diluted from a 500× stock concentration in DMSO) or medium containing a matching concentration of DMSO for 30 min before addition of 0.6% 1-butanol for 30 min. For the time-course study monitoring phosphatidyl butanol (Ptd-But) production, cells were preincubated with increasing amounts of Inh₁ for PLD₁ and Inh₂ for PLD₂ for 10, 20, 30, or 60 min followed by a 30-min incubation with 0.6% 1-butanol.

Both endogenous and exogenous (PLD₂ in AAV vector) human PLD₂ hydrolytic activity cleaving PC to PA product *in vivo* was analyzed by using methods modified from previously described *in vivo* kinetic studies (18,21). Briefly, a fluorescent PA sensor consisting of enhanced GFP fused to a 40-amino acid PA-binding domain from the yeast Spo20

protein was utilized GFP-Spo20-PABD or the mutant GFP-Spo20-PABD-L67R that does not bind PA (21,24–27). Fluorescent intensity generated from the PA sensor and mutant sensor was tracked by lysing the cells with a sonicator at 50% duty cycle and sucrose gradient ultracentrifugation to separate the nuclei of cells from the plasma membrane (and endosomes). A total lipid extraction procedure on the harvested ultracentrifuged fractions (Nuclear and cell membrane portions separated) of the whole cells was performed (nuclear and cell membrane portions separated before lipids were extracted from each) (24,25). Quantitative analysis of fluorescent intensity on a Perkin-Elmer fluorometer (Model LS-45) was performed (24–27). Fluorescent intensity was reported after normalizing for endogenous PLD activity for HEK-293 cells that were transfected when appropriate. Endogenous PLD activity was also measured and PA production quantified with ^{31}P NMR. HEK-293 cells were cultured in small flasks and serum-starved overnight before incubation with 500 nM Inh_2 for 60 min before the addition of 150 ng/mL PMA. Cells were incubated for a further 60 min, then washed in ice-cold PBS, and scraped into ice-cold methanol. Lipids were extracted using acidified organic solvents. Dried lipid extracts were resuspended in methanol, and an aliquot was removed for determination of total lipid phosphorous after wet digestion in perchloric acid (23–25). Phosphatidic acid production was then quantified by ^{31}P NMR.

Western blotting and imaging

Cells were lysed by sonication and run on a 12% SDS-PAGE gel. The blots were blocked in 1% dry milk in Tris HCl pH 8.0. Western blotting for primary (antiphospho-ERK and total ERK and antiphospho-AKT and total AKT) were purchased from Sigma-Aldrich and Thermo Scientific (Pierce Protein Biology Products) and used according to recommended protocols from these companies. DyLight conjugated secondary antibodies (DyLight 488) were used for fluorescent detection of proteins.

Fluorescent signals were generated and imaged UVP gel docking and imaging system (www.uvp.com 12/16/13) equipped with a transilluminator, light box, digital camera, and densitometry software (26,27).

Computer docking of inhibitors into PLD-active site

Computer Dockings of the Small Molecules synthesized in this study was carried out into the PLD_{sp}-active site (PDB Code 1VOY). The Autodock4 program suite was used as previously described (28). Inhibitor structures were drawn in ChemDraw and transferred into PRODRG to convert inh.pdb to inh.pdbq for AutoDock (28,29). Three-dimensional coordinates of phospholipase D were downloaded from RCSB. All the experimental ligands were removed from the pocket of interest. The energy-minimized ligand with full charges was loaded into the PRODRG program. The AutoDock4 per-

formed the docking of the ligands to a set of grids describing the target protein. As a control to make sure the docking parameters were accurate, the synthetic product diC₄PA that was in the active site of the PLD_{sp} structure (Figure 3A) (1VOY), was docked into the active site and compared with the actual position of that product in the crystal structure. AutoDock4 studies resulted in docking scores. Once experimental IC₅₀'s were determined; output files and docking scores were analyzed for comparison with actual kinetic data obtained and log coordinates were converted to output.pdb to produce figures of the most potent inhibitors or if not potent, to illustrate how the molecule may be modified to increase potency for that category of molecules (Table 2 and Figure 3C).

Results and Discussion

Synthesis of inhibitors and testing of PLD_{Sc} and PLD_{Sp} PLD kinetic assay with monomeric substrate diC₄PC and [choline-methyl- ^3H]di-palmitoylPC vesicles to screen potential PLD inhibitors

All inhibitors were synthesized in good yields as depicted in Scheme 1 (6,14). Nineteen compounds were prepared for the biochemical assays. The identification and purity determination were carried out by mass spectrometry and NMR spectroscopy (^1H and ^{13}C). Details of chemical characterization can be found in Appendix S1.

All small molecules synthesized were initially evaluated for their ability to inhibit PLD activity with enzyme from *S.* species strain pmf (PLD_{Sp}) in the pH-stat assay using a synthetic substrate diC₄PC as previously described (1,11,19). PLD activity assay measuring the release of [methyl- ^3H] choline from [choline-methyl- ^3H]di-palmitoylphosphatidylcholine ([choline-methyl- ^3H]PC) vesicles was used as previously described (17,19,20). Once the PLD_{Sp} was prepared, the enzyme was tested with the commercially available PLD inhibitors to demonstrate that the bacterial enzyme, which is readily available to purchase from EnzoLifeSciences, has cross-reactivity with the human PLDs. The results are summarized in Table 1. PLD_{Sp} was inhibited by Inh_VU0155056 and Inh_VU0359595 (a PLD₁ specific inhibitor) with IC₅₀'s of 125 and 50 nM, respectively. PLD_{Sp} also exhibited inhibition with FIPI, a potent commercially available modified halopemide PLD_{1/2} inhibitor. The IC₅₀ for FIPI with PLD_{Sp} was 100 nM (18). Like the human PLDs, PLD_{Sp} is a member of the PLD superfamily and performs both hydrolyase and transferase activities. This is consistent with a mechanism that proceeds through a covalent phosphatidylhistidyl intermediate where the rate-limiting step is formation of the covalent intermediate.

Human recombinant PLD₁ exhibited an IC₅₀ of 255 nM with Inh_VU0155056 reported to be the dual PLD₁ and PLD₂ inhibitor (Table 1). The FIPI inhibitor was 10-fold



Table 1: Comparison of IC₅₀'s of bacterial and human PLDs with commercially available PLD inhibitors and [choline-methyl-³H] labeled di-palmitoylPC vesicles as substrate (15–20)

	Human PLD ₁ ^a (nM)	Human PLD ₂ ^a (nM)	PLD _{Sp} ^a (nM)
PLD enzyme			
Inh_VU0155056 IC ₅₀ ^b	255	225	125
Inh_VU0359595 IC ₅₀ ^b	36	1200	50
Inh_VU0285655-1 IC ₅₀ ^b	>1000	450	1225
FIPI_HCl ^c	25	15	100

^aHuman PLD₁ and PLD₂ sequences were purchased.

^bAll data reported here use the following inhibitors purchased from Avanti Polar Lipids: Inh_VU0359595 is a PLD₁-specific inhibitor and Inh_VU0285655-1 is PLD₂ specific.

^cFIPI was purchased from Sigma-Aldrich and used as a control for successful.

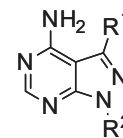
more potent than Inh_VU0155056 for PLD₁ exhibiting an IC₅₀ of 25 nM. FIPI is even more potent than the PLD₁-specific inhibitor from Avanti Polar Lipids Inh_VU0359595 which exhibited an IC₅₀ of 36 nM for PLD₁ (Table 1). The human recombinant PLD₂ enzyme activity IC₅₀ was 225 nM by dual PLD Avanti inhibitor Inh_VU0155056. Interestingly, the PLD₁-specific inhibitor Inh_VU0359595 inhibited PLD₂ in the low micromolar range. The PLD₂-specific inhibitor exhibited an IC₅₀ of 450 nM with PLD₂.

As shown in Table 2, the structure–activity relationship (SAR) studies indicated that all 1,3-disubstituted-4-aminopyrazolopyrimidines showed potency in the low-nanomolar to low-micromolar range for the inhibition of PLD_{Sp} and human PLDs. In general, the potency of inhibition was dependent on the bulkiness of the substituent on 1- and 3- positions R² and R¹, respectively, and the polarity of the R² position (Table 2). For PLD_{Sp}, larger groups (2-naphthyl or 1-naphthyl) as R¹ resulted in a trend toward higher potency. More specifically, when comparing Inh₁ and Inh₂ IC₅₀s for PLD_{sp}, the R² group is playing a larger role for potency. The ability to hydrogen bond in the R² position dominates over bulkiness for the R¹ position. The observation that substituents at R² that are polar and can form hydrogen bonds (O, N or F atoms), such as entry **1** in Table 2, may be the most potent inhibitors of the PLD enzymes for this new class of inhibitors gives us clues as to what the second generation of inhibitors should look like. The next generation of inhibitors to be developed may be with fluorocarbons at this position as in the literature fluorocarbons have been known to be potent inhibitors.

PLD₁ shows highest potency for Inh₁ like PLD_{sp} with an IC₅₀ of 5 nM 4- to 20-fold lower than the next best two inhibitors. Inh₁ was used for the *in vivo* studies with this enzyme. In contrast, PLD₂ exhibited highest potency with

Table 2: Structure–activity relationship for the inhibition of PLD enzymes determined by using both monomer substrate DiC₄PC and [choline-methyl-³H] labeled di-palmitoylPC vesicles

Group	Inhibitor	R ¹	R ²	PLD ₁	PLD _{sp}	PLD ₂
I	1	1-naphthyl	4-MeO-Ph	5	10	125
	2	phenyl	4-MeO-Ph	250	275	15
II	3	2-naphthyl	<i>tert</i> -butyl	500	375	150
	4	1-naphthyl	<i>tert</i> -butyl	426	385	350
	5	phenyl	<i>tert</i> -butyl	550	650	290
	6	methyl	<i>tert</i> -butyl	350	790	1300
III	7	1-naphthyl	2-Et-phenyl	1200	390	1500
	8	phenyl	2-Et-phenyl	1500	450	1250
	9	2-naphthyl	2-Et-phenyl	1550	355	1375
IV	10	1-naphthyl	phenyl	875	545	675
	11	phenyl	phenyl	1250	700	1050
	12	methyl	phenyl	900	1500	120
V	13	1-naphthyl	methyl	20	800	2300
	14	phenyl	methyl	620	695	150
	15	2-naphthyl	methyl	250	650	1200
	16	methyl	methyl	150	1200	1500
VI	17	phenol	H	–	1950	–
	18	2-naphthyl	H	–	1750	–
	19	methyl	H	500	1550	1250



Inh₂ with an IC₅₀ of 15 nM. Smaller trends are also useful when designing second-generation inhibitors. Chemically 1-naphthyl as an R¹ group and 4-MeO-Ph as an R² group has the most potent inhibition for PLD₁ enzyme (Inh₁). The second most potent inhibitor is 1-naphthyl as R¹ group with methyl as R² group. The third most potent is methyl groups in both R¹ and R².

The most effective inhibitor for PLD₂ has a phenyl group at R¹ and 4-MeO-Ph group at R². As with PLD₁, a hydrogen-bonding atom in R² makes a large difference in inhibitor potency. Second best is methyl as R¹ and phenyl as R² (Inh₁₂). The third best is IC₅₀ of 125 nM (Inh₁) with R¹ naphthyl and 4-MeO-Ph as R². Second-generation inhibitors might include a methyl as an R¹ group and 4-MeO-Ph as R² might make a really potent inhibitor.

PLD NMR activity assay on phospholipids in monomer, micelles, SUV vesicles and mixed micelles at 37 °C with +/- PLD inhibitors

Once small molecules that were potent inhibitors of PLD activity were identified by synthetic short-chain phospholipids

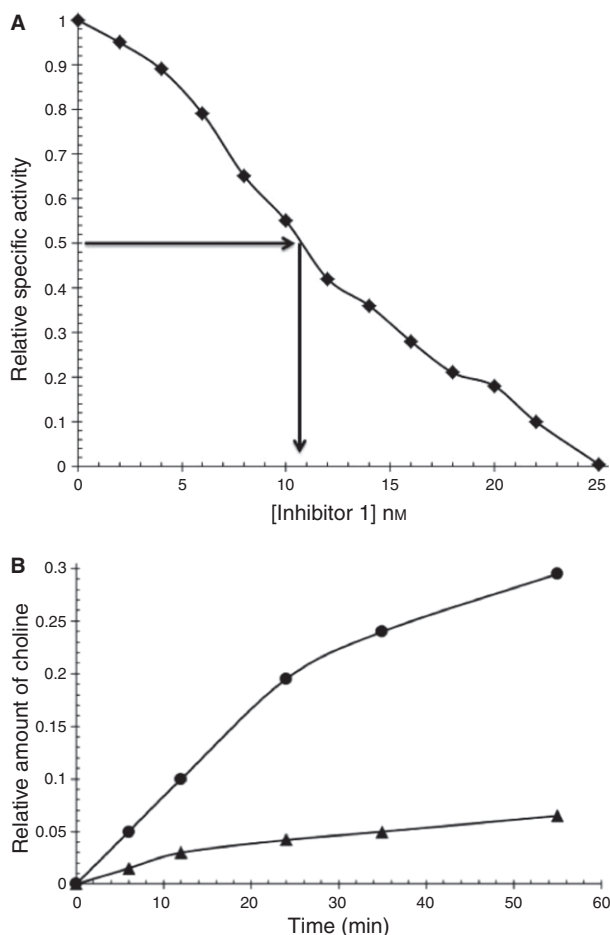


Figure 2: Effect of Inhibitor 1 on PLD_{sp} (A) with monomer diC₄PC pH state assay showing a sample of data from a pH stat assay run in duplicate in the presence of 5 mM diC₄PC and increasing amount of Inhibitor 1 in the nanomolar range. All data points were run in duplicate. Error for duplicate data points was between 15% and 20% (B) Choline production monitoring hydrolysis of 1-palmitoyl-2-oleoyl-PC (POPC) unilamellar vesicles as substrate with ¹H Spectra. The formation of free choline was monitored to calculate specific activity as previously described (17,18,21) using 10 mM POPC vesicles in 25 mM imidazole pH 7.0 here in the absence (circles) and presence (Triangles) of Inhibitor 1. All data were collected in duplicate experiments, and experimental error was between 15% and 20%.

(Table 2 and Figure 2a), further kinetic studies were carried out on vesicles using ³¹P and ¹H NMR. NMR studies have been established as the preferred method to measure PLD activity with vesicles instead of pH-stat assays with vesicles due to the high pK_{a2} of PA in vesicles (pK_{a2} of 7.6 in predominantly PC bilayers increasing as PA increases) which makes pH-stat assays of PLD-mediated cleavage of PC to PA problematic because at an end-point of 8.0 only part of the PA is titratable. ¹H NMR spectroscopy was used to monitor PLD activity by measuring the intensity of the water-soluble choline *N*-methyl resonance as previously described in detail (19,20). Briefly, chemical shifts of 3.15

and 3.18 ppm were used to monitor inner and outer leaflet of PC in SUV and the emergence of free choline at ~3.09 ppm (16,19). Although overall we had slightly higher (20–30%) specific activities than previously reported for these NMR assays for PLD_{Sp} [See Table 3 and references (20)], many of the trends previously published for monomer and vesicle kinetics were reproduced for these inhibitor studies. As shown in Figure 2B, the hyperbolic kinetics of PLD activity toward POPC previously described was reproduced in the absence (and presence) of PLD inhibitor **1** from Table 2. The inhibitory effects of Inh_1 reduced activity of the PLD enzymes to 1–5% or original activity for monomeric substrates and <10% for vesicle substrates (Figure 2B and Table 3).

Inh_1 chosen for NMR kinetic and vesicle binding studies showed high potency in the low-nanomolar range with both the monomeric pH-stat and vesicle kinetic assay (Table 2) had to be used in concentrations in the median-nanomolar range ~300 nM (Table 3) to get significant inhibitory effects (~3–4 times more concentrated). This may be partly due to the fact that phospholipases have a unique obstacle that complicates kinetics relative to other enzymes in that to cleave this type of substrate. For every catalytic cycle, enzymes in the phospholipid family must have a mechanism to insert into the leaflets of the bilayer, extract monomer substrate from the lipid bilayer, cleave the monomer to products, and then release the products into the lipid bilayer to turnover efficiently. The complexity of the kinetics is reflected in the disparity between the amount of substrate necessary to be presented to the enzyme in vesicle form to reach the apparent *K_m* and *V_{max}*. Due to low yields of some inhibitors, the full vesicle kinetic studies were limited to Inh_1 for PLD_{sp}.

Overall, we had slightly higher (20–30%) specific activities than previously reported for these NMR assays (See Table 3 and references (18,20,21)). Table 3 showed remarkable elimination of transferase activity for the PLD_{sp} enzyme in the presence of inhibitor **1** (negligible transferase activity detected at as low as 50 nM inhibitor concentration). Inhibition of PLD activity toward vesicle substrate was observed to be 2–3-fold less potent overall than monomer substrate. This is probably due in part to the complex mode of binding and catalysis of enzymes that work at the lipid bilayer interface to extract monomer substrate discussed previously. Interestingly, for both NMR and *in vivo* studies, the inhibition of vesicle hydrolysis was much more effective if the enzyme was preincubated for 60–90 min at 37 °C with inhibitor. Directly adding inhibitor and enzyme to the vesicles for these studies resulting in addition of up to 300 nM inhibitor to get the same effect observed with 30–120 nM (with preincubation with PLD enzyme) reported in Table 3. This implies a conformational change may be required in the PLD enzyme to limit binding to the POPC vesicle. It is hoped that a future crystal structure of the PLD/inhibitor

Table 3: PLD_{sp} activity toward phospholipids in monomer, micelles, vesicles, and mixed micelles at 37 °C +/- Inh₁ (inhibitor) using NMR

Substrate	Conc. (mM)	Ca ²⁺ (mM)	Physical state	Specific hydrolase ^a	Activity transferase ^a
diC ₄ PC	5	0	Monomer	0.15 (15.5)	0.00 (10.3)
diC ₆ PC	5	0	Monomer	0.22 (11.5)	0.00 (3.26)
diC ₇ PC	5	0	Micelle	0.58 (8.5)	0.25 (2.96)
POPC	10	5	SUV	0.49 (5.4) ^b	
POPC	10	5	LUV	0.23 (2.10) ^b	
POPC/ chol	5/5	5	SUV	0.44 (5.90) ^{b,c}	
POPC + TX-100	5/20	0	Mixed micelle		5.25 (125) ^d

PA, phosphatidic acid; POPC, 1-palmitoyl-2-oleoyl-PC; SUV, small unilamellar vesicles.

^aHydrolase (generation of PA) and transferase (generation of PG) activities of PLD_{sp} (2.5 ug) toward 5 mM diCnPC with 5 mM glycerol present in 50 mM MES-NaOH buffer, pH 6.5; ³¹P NMR was used to monitor PA and PG production.

^bThe specific activity of the enzyme was measured by ¹H NMR spectroscopy monitoring for choline production. This is known as a combination of hydrolase and transphosphatidyl reaction rates. Duplicate assay samples were used to obtain rates; errors in the rates were between 15% and 20%.

^cThe specific activity is based on the rate over the first 25 min; unlike with pure POPC SUVs, the rate decreased over longer times when cholesterol was present in the vesicles.

^dWith this amount of TX-100 present, the major (>90%) product for PLD_{sp} is the transphosphatidyl product with the Triton molecule (20).

complex will supply information needed to fully interpret these results.

Analysis of docking of small molecules into PLD_{sp}-active site (PDB_ID 1V0Y)

Dibutylphosphatidylcholine (diC₄PC) is the soluble synthetic substrate for PLD (also used in pH-stat assay in this study) that was reacted with the crystallized PLD_{sp} enzyme crystal. The crystallized enzyme actually cleaved the substrate to products choline and 2-butylroxy-1-tetrahydroxyphosphoranyloxy-methyl-ethylbutyrate (diC₄PA) before data were collected for the structure/ligand complex (PDB code 1V0Y) (11) Figure 3A shows the PLD_{sp} enzyme (1V0Y) cocrystallized with diC₄PA. The active site consists of hydrophobic areas to the left and upper right. The short alkyl chains of the diC₄PA product lie toward the hydrophobic region of the interior of the pocket. There are hydrophilic areas of the enzyme below center of gravity of the active site cavity (Asn465, His170, Lys450, Lys172, His448, and Asn187) surrounding the phosphate moiety where the polar portion of this molecule is bonded (Figure 3A). The most potent inhibitor for the PLD_{sp} enzyme is docked as described in experimental methods (inhibitor **1** from Table 2) with IC₅₀ of 10 nM in Figure 3B to look for

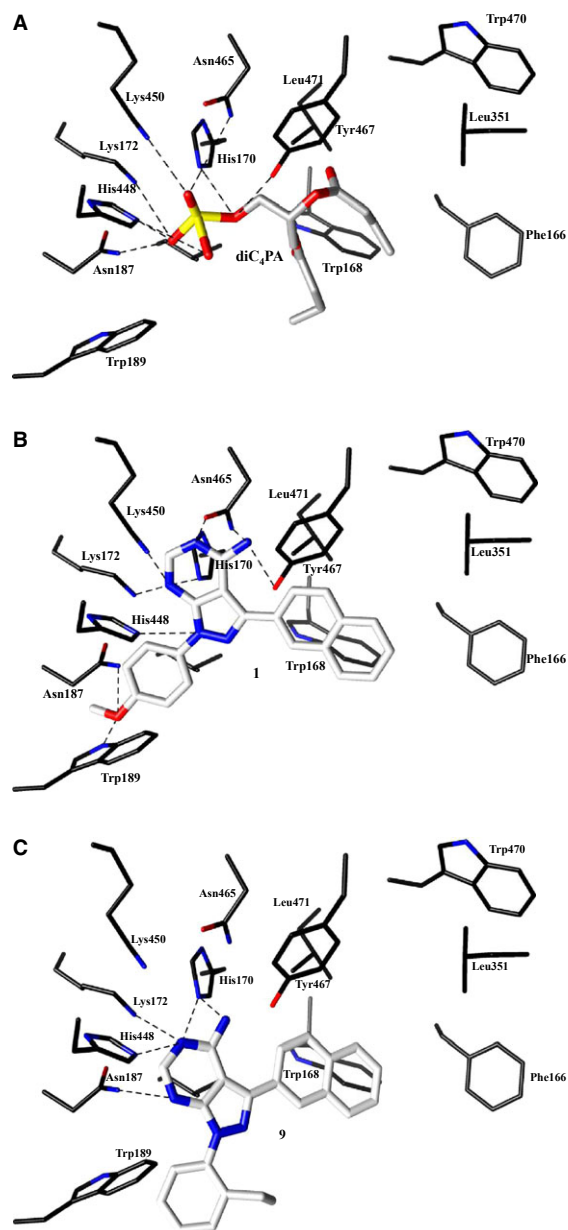


Figure 3: The PDB use for Docking Studies is 1V0Y (S_{sp}. PLD) (A) PLD bound to synthetic product diC₄PA (after being soaked in synthetic substrate diC₄PC) in the crystal structure from RCSB (PDB code 1V0Y) (B) **1** docked in PLD (C) **9** docked in PLD.

possible trends on how these types of inhibitors may bind to the enzyme. The tight binding observed from the actual IC₅₀ may be due to the hydrogen-binding capacity of the oxygen of the R² (4-methoxyphenyl) substituent in the phosphate-binding pocket of the enzyme suggested by the predicted binding in the molecular docking (Figure 3B). In contrast, PLD_{sp} binding to docked **9** is shown in Figure 3C; without hydrogen-binding capacity at R², the IC₅₀ increases to 350 nM. This trend for PLD_{sp} inhibition shows that the R² group of Inh₁ has enhanced inhibitory capacity for the PLD_{sp} enzyme when able to hydrogen

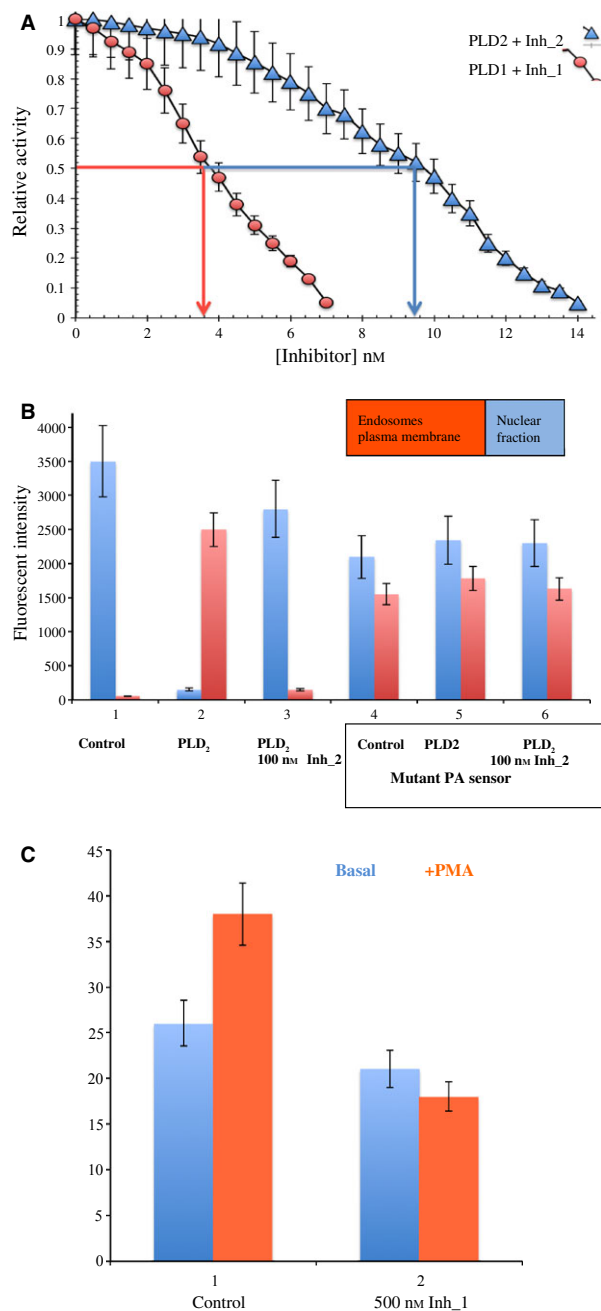


Figure 4: Inh₁ and Inh₂ are potent *in vivo* inhibitors. (A) HEX-293 cell lines were transfected with PLD₁ and PLD₂ constructs overnight, and then once expression confirmed (GFP reporter protein), 0.6% 1-butanol was added, and Ptd-But production was measured to quantify transphosphatidylation reaction. Measurements were taken in triplicate and normalized for any endogenous PLD activity (+/- PMA). Increasing concentrations of Inh₁, Inh₂ or DMSO control were added. (B) Inh₂ blocks translocation of a phosphatidic acid (PA) sensor to the plasma membrane. PLD₂ over-expressing HEX-293 cells (transfected overnight with AAV-GFP-PLD₂ construct) were transfected with the PA sensor GFP-Spo20-PABD or the mutant GFP-Spo20-PABD-L67R that does not bind PA. After the transfection with the PA sensors, cells were viewed under the fluorescent microscope to confirm negative and positive controls were working. Then, after separating nuclei from membrane with ultracentrifugation and total lipid extraction, PA sensor for each subcellular location was quantified on a Perkin-Elmer LS-45 fluorometer. Assays were performed in duplicate. (C) Analysis of PA production in endogenously PLD expressing HEX-293 cells. HEK-293 cells +/- PMA treatment as a positive control. Phosphatidic acid production was evaluated in 500 nM Inh₂. Phosphatidic acid was quantified after total lipid extraction followed by ³¹P NMR.

Inh₂ exhibited potent inhibition of exogenous PLD transphosphatidylation activity. Inh₁ IC₅₀ is ~3.75 nM and Inh₂ IC₅₀ is ~9.5 nM. Figure 4B shows that Inh₂ is a potent *in vivo* inhibitor blocking phospholipid head-group cleavage of PC. When cells are inactive, the majority of the sensors are localized to the nucleus (Figure 4B control group 1). When cells are overexpressing PLD₂, the PA sensor fluorescent intensity was found to increase by about 100-fold in fluorescent intensity within the subcellular plasma membrane fraction, strongly suggesting that more PA was moving into the plasma membrane fraction and to intracellular membrane vesicles (endosomes) colocalized outside the nucleus (Figure 4B compare groups 1 and 2 plasma membrane/endosome subcellular fraction fluorescent intensity). This is known to happen when PLDs are actively generating PA from PC. After addition of 100 nM of Inh₂ to the PLD₂-overexpressing cells, the fluorescent intensity of the nuclear fraction and plasma membrane/endosomes were reversed back to the profile of group 1 with low or no PLD activity in resting cells, indicating a lack of generation of PA by PLD₂. Thus, Inh₂ is a potent inhibitor of head-group hydrolysis of PC to PA. Repeating the assay with the mutant PA sensor indicates a more random distribution of fluorescent intensity between the plasma membrane and nuclear fractions analyzed (negative controls Figure 4B Groups 4, 5, and 6). Endogenous activity of PLD₂ is increased by stimulating HEK-293 cells with PMA. Figure 4C group 1 shows endogenous PLD activity (relative PA levels) nearly 30% higher in the presence of PMA. As shown in Figure 4C group 2, treatment of HEK293 cells with 500 nM Inh₂ blocks both endogenous and PMA stimulated PLD activity (PA production by dropping relative levels of PA by 20% without PMA stimulation and over 50% in PMA-stimulated cells comparing groups 1 and 2 in Figure 4C).

bond to polar side chains in the phosphate-binding pocket. (Table 2: compare **1** and **9** and Figure 3B,C).

In vivo transphosphatidylation and head-group hydrolysis (PA production) kinetic assays

Figure 4A measures Inh₁ and Inh₂ capacity to inhibit PLD transphosphatidylation by measuring the production of Ptd-But. HEX-293 cells overexpressing PLD₁ or PLD₂ were incubated with increasing amounts of Inh₁ or Inh₂, respectively, or DMSO control before addition of 0.6% 1-butanol. As seen in Figure 4A, both Inh₁ and

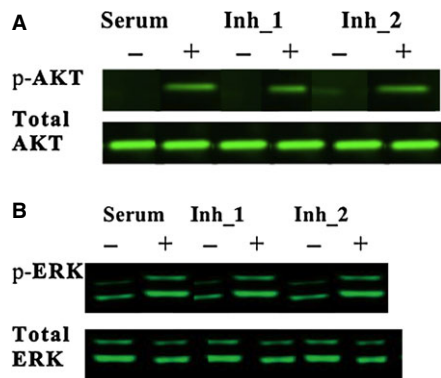


Figure 5: PLD Inhibitors Inh₁ and Inh₂ do not alter upstream signaling events. Inh₁ and Inh₂ do not effect AKT phosphorylation upon serum stimulation. MDA-MB-231 cells were starved overnight before being pretreated with 500 nM Inh₁ or Inh₂ or DMSO (control) for 12 h and then stimulated with serum for 45 min. Cell lysates were analyzed by SDS-PAGE and Western blotting with antibodies against: (A) phosphorylated AKT, total AKT, and (B) phosphorylated ERK, or total ERK.

Inh₁ and Inh₂ do not affect PLD subcellular localization, actin stress fiber network in resting HEK-293 cells and do not affect signaling events upstream from PLD activation

There are molecules known to dislocate PLDs from the plasma membrane where they are associated when PLD is active. This would be indirect inhibition. Patterns in actin fibers viewed through the fluorescent microscope did not show visual differences when comparing cells used in these *In vivo* kinetic assays over-expressing human PLD₁ and PLD₂ in the presence and absence of Inh₁ and Inh₂ (data not shown). As PLD activation has been reported in the literature to occur downstream of cell signaling events such as AKT and/or ERK activation (18), examination of phosphorylated and total AKT and ERK was performed with Western blot analysis in the presence and absence of Inh₁ and Inh₂. As shown in Figure 5A,B, serum-starved cells did not express high levels of phosphorylated AKT and ERK. The presence of serum stimulates phosphorylation of AKT and ERK. Comparing lanes 2, 4, and 6 for phosphorylated AKT and ERK (p-AKT and p-ERK), the presence of 500 nM of either Inh₁ or Inh₂ for 12 h does not significantly alter the expression of the phosphorylated form of these signaling molecules. This is strong evidence that these PLD inhibitors act specifically on the PLD enzyme in these *in vivo* assays.

Conclusions

In conclusion, a diverse set of substituted pyrazolopyrimidines have been prepared in a five-step synthesis. These compounds were tested for the inhibition of PLD_{Sp} and human PLD₁ and PLD₂ enzymes initially using the pH-stat assay, followed by a standard PLD kinetic assay measuring

the release of [methyl-³H] choline from [choline-methyl-³H] di-palmitoylphosphatidylcholine ([choline-methyl-³H]PC) vesicles as previously described (18,21). For PLD_{sp}, the hydrophobicity of the active site requires some 'bulk' at position R² comparing inhibitors **18** (no bulk at R²) with **2**, **9**, and **15** (Table 2). The most potent inhibitors for PLD_{sp} would be those that have some hydrophobicity at R² and are not too bulky, yet can engage in hydrogen bonding as shown with **1** (Table 2 and Figure 3B). NMR vesicle kinetic assays were also performed. For the recombinant human PLD₁ and PLD₂ enzymes, Inh₁ and Inh₂ molecules were used in the *in vivo* cell-based kinetic assays. In the transphosphatidylase kinetic assay (increase of Ptd-But product) *in vivo*, Inh₁ and Inh₂ exhibited IC₅₀'s of approximately 3.75 and 8.5 nM with PLD₁ and PLD₂, respectively (Figure 4A). For *in vivo* head-group cleavage assay, a PA product-tracking molecule was utilized. Results of subcellular fractionation separating nuclei from plasma membrane and analysis of total lipids of each fraction showed that Inh₂ was very potent (100 nM) at preventing the translocation of the PA tracker from the nucleus to the cytoplasm and intracellular vesicles, which happens when PA product builds up in the absence of the inhibitor (18). There was remarkable consistency between the *in vitro* and *in vivo* assays, which have physiological relevance. The docking studies using AutoDock4 suggested that the naphthyl group as R¹ lies in the hydrophobic region of the pocket but there is room for expansion or elongation to go deeper into the pocket (more like the alkyl chains of phospholipids (Figure 3B,C). Overall, the exogenous inhibition and *in vivo* inhibition observed with some of the novel molecules in this study are at least as potent as previously reported specific and highly effective inhibitors to mammalian PLD tested in both cell-based and *in vitro* assays.

Acknowledgments

Financial help from University of Massachusetts Boston and technical support from Roxbury Community College Biotechnology Program are gratefully acknowledged. KS would like to thank Feng Wang formerly of Boston University for helpful discussions about molecular modeling of the binding of enzyme/lipid bilayers for follow-up and future studies and the technical staff at Boston University's Chemical Instrumentation Center (CIC) for their assistance with NMR to complete some of these kinetic studies. A special thanks to Vicky Curry formerly of RCC, now at Dana Farber Cancer Institute for all her extra work on this project. Also, thanks to the laboratory staff in Pediatric Oncology to prepare the PA fluorescent probes (wild type and mutant) and the CHO PLD-inducible cell line and to maintain the MDA-MB-231 cells for the Western blotting experiments for this study. Thanks to Dr. Polina Anikeeva and Ritchie Chen of MIT Center of Material Sciences and Engineering for their time training me in molecular biology techniques in Dr. Anikeeva's RET program (summer 2013)

and for donating the original AAV-gCAMP vector, HEX-293 cells and enzymes used to prepare the PLD1 and PLD2 constructs with Green Fluorescent Protein (GFP). Thanks to Mark R. Payne and Julie V. Charbeneau for their excellent editorial skills and summary of PLD₁ and PLD₂ trends for *in vitro* inhibition (Table 2).

References

- Brown H.A., Henage L.G., Preininger A.M., Xiang Y., Exton J.H. (2007) Biochemical analysis of phospholipase D. *Methods Enzymol*;434:49–87.
- Foster D.A. (2009) Phosphatidic acid signalling to mTOR: signals for the survival of human cancer cells. *Biochim Biophys Acta*;1791:949–955.
- Zhao Y., Ehara H., Akao Y., Shamoto M., Nakagawa Y., Banno Y., Deguchi T., Ohishi N., Yagi K., Nozawa Y. (2000) Increased activity and intranuclear expression of phospholipase D2 in human renal cancer. *Biochem Biophys Res Commun*;278:140–143.
- Uchida N., Okamura S., Kuwano H. (1999) Phospholipase D activity in human gastric carcinoma. *Anticancer Res*;19:671–676.
- Yamada Y., Hamajima N., Kato T., Iwata H., Yamamura Y., Shinoda M., Suyama M., Mitsudomi T., Tajima K., Kusakabe S., Yoshida H., Banno Y., Akao Y., Tanaka M., Nozawa Y. (2003) Association of a polymorphism of the phospholipase D(2) gene with the prevalence of colorectal cancer. *J Mol Med*;81:126–131.
- Scott S.A., Selvy P.E., Buck J.R., Cho H.P., Criswell T.L., Thomas A.L., Armstrong M.D., Arteaga C.L., Lindsley C.W., Brown H.A. (2009) Design of isoform-selective phospholipase D inhibitors that modulate cancer cell invasiveness. *Nat Chem Biol*;5:108–117.
- Jin J.K., Ahn B.H., Na Y.J., Kim J.I., Kim Y.S., Choi E.K., Ko Y.G., Chung K.C., Kozlowski P.B., Mindo S. (2007) Phospholipase D1 is associated with amyloid precursor protein in Alzheimer's disease. *Neurobiol Aging*;28:1015–1027.
- Oliveira T.G., Di Paolo G. (2010) Phospholipase D in brain function and Alzheimer's disease. *Biochim Biophys Acta*;1801:799–805.
- Lewis J.A., Scott S.A., Lavieri R., Buck J.R., Selvy P.E., Stoops S.L., Armstrong M.D., Brown H.A., Lindsley C.W. (2009) Design and synthesis of isoform-selective phospholipase D (PLD) inhibitors. Part I: impact of alternative halogenated privileged structures for PLD1 specificity. *Bioorg Med Chem Lett*;19:1916–1920.
- Lavieri R., Scott S.A., Lewis J.A., Selvy P.E., Armstrong M.D., Brown H.A., Lindsley C.W. (2009) Design and synthesis of isoform-selective phospholipase D (PLD) inhibitors. Part II: identification of the 1, 3, 8-triazaspiro[4,5]decan-4-one privileged structure that engenders PLD2 selectivity. *Bioorg Med Chem Lett*;19:2240–2243.
- Leiros I., Mcsweeney S., Hough E. (2004) The reaction mechanism of phospholipase D from *Streptomyces* sp strain PMF. Snapshots along the reaction pathway reveal a pentacoordinate reaction intermediate and an unexpected final product. *J Mol Biol*;339:805–820.
- Bishop A.C., Kung C., Shah K., Witucki L., Shokat K.M., Liu Y. (1999) Generation of onospecific nanomolar tyrosine kinase inhibitors via a chemical genetic approach. *J Am Chem Soc*;121:627–631.
- Apfel B., Blair J.A., Gonzalez B., Nazif T.M., Feldman M.E., Aizenstein B., Hoffman R., Williams R.L., Shokat K.M., Knight Z.A. (2008) Targeted polypharmacology: discovery of dual inhibitors of tyrosine and phosphoinositide kinases. *Nat Chem Biol*;4:691–699.
- Hanefeld U., Rees C.W., White J.P., Williams D.J. (1996) One-pot synthesis of tetrasubstituted pyrazoles-proof of regiochemistry. *J Chem Soc Perkin Trans*;1:1545–1552.
- Geng D., Baker D.P., Foley S.F., Zhou C., Stieglitz K., Roberts M.F. (1999) A 20-kDa domain is required for phosphatidic acid-induced allosteric activation of phospholipase D from *Streptomyces chromofuscus*. *Biochim Biophys Acta*;1430:234–244.
- Stieglitz K., Seaton B., Roberts M.F. (1999) The role of interfacial binding in the activation of *Streptomyces chromofuscus* phospholipase D by phosphatidic acid. *J Biol Chem*;274:35367–35374.
- Stieglitz K.A., Seaton B., Roberts M.F. (2001) Binding of proteolytically processed phospholipase D from *Streptomyces chromofuscus* to phosphatidylcholine membranes facilitates vesicle aggregation and fusion. *Biochemistry*;40:13954–13963.
- Su W., Yeku O., Olepu S., Genna A., Park J.S., Ren H., Du G., Gelb M.H., Morris A.J., Frohman M.A. (2009) 5-Fluoro-2-indolyl des-chlorohalopemide (FIPI), a phospholipase D pharmacological inhibitor that alters cell spreading and inhibits chemotaxis. *Mol Pharmacol*;75:437–446.
- Geng D., Chura J., Roberts M.F. (1998) Activation of PLD by phosphatidic acid: enhanced vesicle binding, phosphatidic acid-Ca²⁺ interaction, or an allosteric effect? *J Biol Chem*;273:12195–12202.
- Yang H., Roberts M.F. (2003) Phosphohydrolysis and transphosphatidyl transfer reactions of two *Streptomyces* phospholipase D enzymes: covalent versus non-covalent catalysis. *Protein Sci*;12:2087–2098.
- Hammond S.M., Altshuler Y.M., Sung T.C., Rudge S.A., Rose K., Engebrecht J., Morris A.J., Frohman M.A. (1995) Human ADP-ribosylation factor-activated phosphatidylcholine-specific phospholipase D defines a new and highly conserved gene family. *J Biol Chem*;270:29640–29643.
- Su W., Chardin P., Yamazaki M., Kanaho Y., Du RhoA-mediated G. (2006) Phospholipase D1 signaling is not required for the formation of stress fibers and focal adhesions. *Cell Signal*;18:469–478.
- Du G., Huang P., Liang B.T., Frohman M.A., MA, (2004) Phospholipase D2 localizes to the plasma mem-



brane and regulates angiotensin II receptor endocytosis. *Mol Biol Cell*;15:1024–1030.

24. Morris A.J., Frohman M.A., Engebrecht J. (1997) Measurement of phospholipase D activity. *Anal Biochem*;252:1–9.
25. Zeniou-Meyer M., Zabari N., Ashery U., Chasserot-Golaz S., Haeberle A.M., Demais V., Bailly Y., Gottfried I., Nakanishi H., Neiman A.M., Du G., Frohman M.A., Bader M.F., Vitale N. (2007) Phospholipase D1 production of phosphatidic acid at the plasma membrane promotes exocytosis of large dense-core granules at a late stage. *J Biol Chem*;282:21746–21757.
26. Kang J.H., Chung J.K. (2008) Molecular-genetic imaging based on reporter gene expression. *J Nucl Med*;49:164S–179S.
27. Jung A.C., Crique M.C., Rutschmann S., Hoffmann J.A., Ferrndon D. (2001) Microfluorometer assay to measure the expression of beta-galactosidase and green fluorescent reporter genes in single *Drosophila* flies. *Biotechniques*;30:594–598, 600-1.
28. Morris G.M., Goodsell D.S., Halliday R.S., Huey R., Hart W.E., Belew R.K., Olsen A.J.J. (1998) Automated docking using a Lamarckian genetic algorithm and empirical binding free energy function. *Comput Chem*;19:1639–1662.
29. Schüttelkopf A.W., van Aalten D.M.F. (2004) A tool for high-throughput crystallography of protein-ligand complexes. *Acta Crystallogr D Biol Crystallogr*;D60:1355–1363.

Supporting Information

Additional Supporting Information may be found in the online version of this article:

Appendix S1. ^1H and ^{13}C NMR spectra of the molecules synthesized for PLD Inhibitor Studies.